

## Accepted Manuscript

TEMPO-mediated Aerobic Oxidation of Alcohols using Copper(II) Complex of Bis(phenol) di-amine Ligand as Biomimetic model for Galactose oxidase Enzyme

Elham Safaei, Leila Hajikhanmirzaei, Babak Karimi, Andrzej Wojtczak, Patricia Cotič, Yong Lee

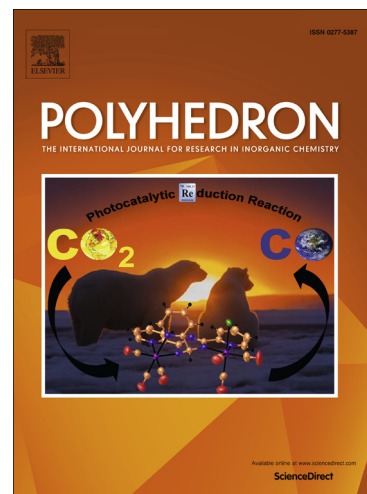
PII: S0277-5387(15)00660-9  
DOI: <http://dx.doi.org/10.1016/j.poly.2015.11.003>  
Reference: POLY 11647

To appear in: *Polyhedron*

Received Date: 16 June 2015  
Accepted Date: 4 November 2015

Please cite this article as: E. Safaei, L. Hajikhanmirzaei, B. Karimi, A. Wojtczak, P. Cotič, Y. Lee, TEMPO-mediated Aerobic Oxidation of Alcohols using Copper(II) Complex of Bis(phenol) di-amine Ligand as Biomimetic model for Galactose oxidase Enzyme, *Polyhedron* (2015), doi: <http://dx.doi.org/10.1016/j.poly.2015.11.003>

This is a PDF file of an unedited manuscript that has been accepted for publication. As a service to our customers we are providing this early version of the manuscript. The manuscript will undergo copyediting, typesetting, and review of the resulting proof before it is published in its final form. Please note that during the production process errors may be discovered which could affect the content, and all legal disclaimers that apply to the journal pertain.



**TEMPO-mediated Aerobic Oxidation of Alcohols using  
Copper(II) Complex of Bis(phenol) di-amine Ligand as  
Biomimetic model for Galactose oxidase Enzyme**

Elham Safaei<sup>\*a,b</sup>, Leila Hajikhanmirzaei<sup>b</sup>, Babak Karimi<sup>b</sup>,  
Andrzej Wojtczak<sup>c</sup>, Patricia Cotič<sup>d</sup>, Yong Lee<sup>e</sup>

<sup>a</sup>Department of Chemistry, College of Sciences, Shiraz University, Shiraz, 71454, Iran

<sup>b</sup>Institute for Advanced Studies in Basic Sciences (IASBS), 45137-66731, Zanjan, Iran

<sup>c</sup>Nicolaus Copernicus University, Department of Chemistry, 87-100, Torun, Poland

<sup>d</sup>Institute of Mathematics, Physics and Mechanics, Jadranska 19. SI-1000, Ljubljana, Slovenia

<sup>e</sup>Department of Chemistry, Changwon National University, Changwon 641-773, South Korea

Correspondence to: Elham Safaei

E-mail:safaei@iasbs.ac.ir

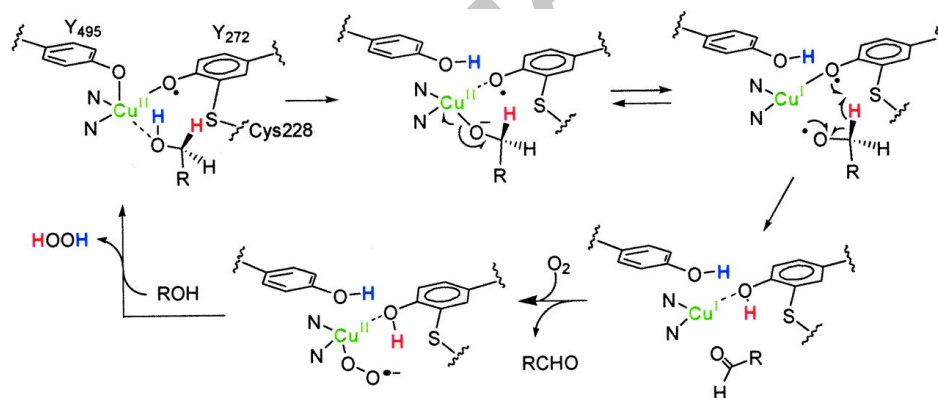
**Abstract**

Mononuclear copper complexes of four-dentate N<sub>2</sub>O<sub>2</sub> bis(phenol) diamine ligands (H<sub>2</sub>L<sup>NEX</sup> X: C and OB in which C and OB are chloro and *tert*-butyl- methoxy substituents on phenol groups) have been synthesized and characterized by IR, UV-Vis, single crystal X-ray diffraction, magnetic susceptibility studies and cyclic voltammetry techniques. The CuL<sup>NEX</sup> complexes show the square pyramid geometry of the coordination sphere with the copper centres surrounded by two nitrogen and oxygen atoms from the coordinating ligand and an axially bound water molecule. The effective magnetic moments of 1.7 and 1.8 B.M confirm a monomer complex with copper(II) center. Electrochemical oxidation of these complexes yielded the corresponding Cu(II)-phenoxyl radical species. In addition, CuL<sup>NEX</sup> complexes, have shown efficient catalytic activities for TEMPO-mediated oxidation of a set of alcohols to the corresponding aldehydes in the presence of molecular oxygen as oxidant at room temperature.

**Keywords:** GOase; Biomimetic copper complexes; Phenoxyl radical; Alcohol oxidation; TEMPO.

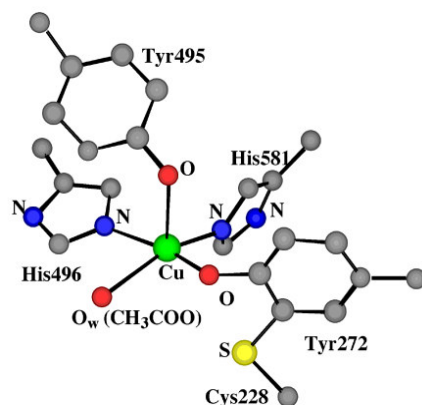
## 1. Introduction

Nature has invented many efficient enzymes able to assist in performing certain, necessary reactions with high turnover rates. Many chemical transformations, which require dangerous or expensive chemicals in the lab, also occur in nature under environmentally friendly conditions by the enzyme catalysis. Oxidases are one of the most important enzymes that catalyze oxidation of a substrate. These enzymes are subgroups of the oxidoreductase class that catalyze an oxidation-reduction reaction involving reduction of molecular oxygen ( $O_2$ ) to water ( $H_2O$ ) or hydrogen peroxide ( $H_2O_2$ ) [1,2]. Galactose oxidase (GOase) is a member of the family of radical-coupled copper oxidases of fungal origin (Schemes 1, 2) that catalyze two-electron oxidation of primary alcohols into aldehydes, with reduction of dioxygen into hydrogen peroxide [3, 4].



**Scheme 1.** Active site for GOase and proposed mechanism for catalysis by GOase [4]

The structure of this biomolecule is well established (Scheme 2) [5, 6]. The crystal structure of GOase contains a square-pyramidal copper ion with a tyrosinate ligand weakly bound in the axial position, two histidine imidazole units, a second tyrosinate and either  $H_2O$  or acetate (replacing the substrate) in the equatorial sites (Scheme 2) [7-14]. An axial tyrosine (Tyr475) manages the proton transfer occurring during catalysis [8-13].

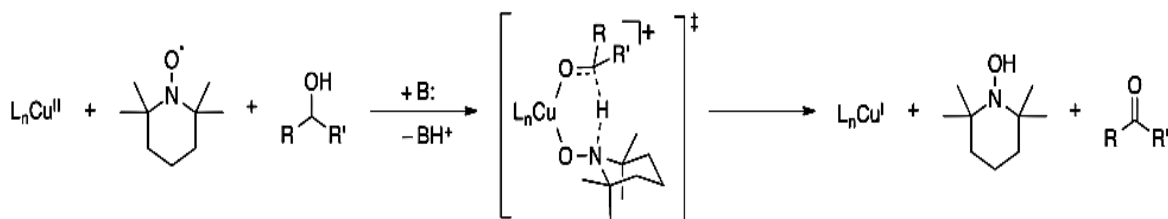


**Scheme 2.**Galactose oxidase (GOase)active site [14]

Active site of GOase is an important part of this enzyme as well as other enzymes, providing structural, catalytic and electron transfer functions. Reproducing this active site in an enzyme model in order to better understand the GOase structure and function and develop new catalysts has been one of the most important challenges in the field of bio-inorganic chemistry [15-19].

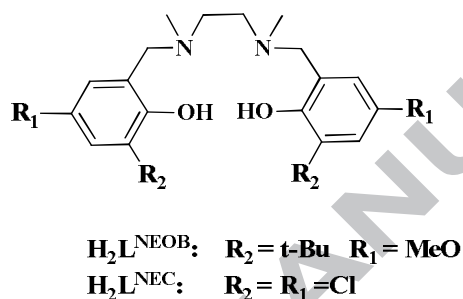
The catalytic oxidation of alcohols into corresponding carbonyl compounds is one of the most fundamental reactions in organic chemistry [20–22]. In 1977, for the first time, a ligand–assisted Cu catalytic system comprising copper with pyridine (py) or bipyridine (bipy) ligands [23] was reported to catalyze the selective oxidation of alcohols to aldehydes using  $O_2$  as final oxidant. A few decades later, the catalytic activity of other N-containing ligands such as 1,10–phenanthroline (phen) or TMEDA–assisted Cu systems was re-investigated [24]. The catalytic oxidation of alcohols to aldehydes based on the isolated Cu complexes has been also reported by several groups [25-28]. The first synthesized Cu complex system, which may be considered as the functional model of GOase, efficiently catalyzes the oxidation of alcohols to aldehydes under  $O_2$  pressure at 25 °C [29]. Other scientists have been successfully imitating the active form of the natural enzyme GOase in numerous model complexes [30-41]. The most well-known alcohol oxidation studies by aminophenol, imine

type ligands copper complexes have been reported by Wieghardt, Stacks, Timo and Fabbrini groups [42-45]. Nitroxyl radicals are known to act as radical scavenging antioxidants. They are extremely popular in various fields of science and technology [46]. Particularly, they have found wide applications as oxidation catalysts [47, 48]. TEMPO (2,2,6,6-tetramethylpiperidinyloxy) is a well-known nitroxyl radical which may oxidize a number of functionalities [49–56]. Most of the studies on this stable radical have been reported for the transformation of alcohols to the corresponding carbonyl compounds [54–59]. Only a few groups have reported catalytic systems involving TEMPO in combination with transition metals such as Ru [60] and Cu [62, 63] as co-catalysts for the oxidation of alcohols using molecular oxygen or air under mild reaction conditions. The first copper/nitroxyl radical catalyzing oxidation has been reported in 1984 by Semmelhack *et al.* [62], who managed to oxidize allylic and benzylic alcohols at room temperature in DMF. Despite many reports on oxidation of alcohols to aldehydes, reports on this organic transformation using copper(II) complexes in the presence of TEMPO are scarce [62]. Stahl group [63] has summarized their contributions to the development and/or mechanistic characterization of a series of different Cu-catalyzed aerobic oxidation reactions. One of the three mechanistic pathways for this reaction involves redox cooperativity between Cu(II) and TEMPO cocatalyst (Scheme 3), which enables highly versatile and efficient alcohol and amine oxidation reactions.



**Scheme 3.** Redox cooperativity with TEMPO co-catalyst [63]

The main focus of this project was to find new  $N_2O_2$  based ligand candidates which could substitute classical bipy and phen with improved catalytic activity for the oxidation of benzylic alcohols. Thus we paid attention to the synthesis of novel mononuclear copper complexes of four-dentate  $N_2O_2$  bis(phenol) diamine ligands [64] and subsequently investigate their performances as efficient catalytic system in combination with TEMPO in the aerobic oxidation of benzylic alcohols (Scheme 4).



**Scheme 4.** Bis(phenol) diamine  $H_2L^{NEX}$  [64]

## 2. Experimental

### 2.1. Materials and physical measurements

Reagents or analytical grade materials were obtained from commercial suppliers and used without further purification, except those for electrochemical measurements. Elemental analyses (C, H, N) were performed by the Isfahan University of Technology. Fourier transform infrared spectroscopy on KBr pellets was performed on a FT IR Bruker Vector 22 instrument. NMR measurements were performed on a Bruker 400 instrument. UV-Vis absorbance digitized spectra were collected using a CARY 100 spectrophotometer. The electronic absorption spectra of complexes have been measured in dichloromethane in the 200-800 nm range.

Crystals for the X-ray diffraction experiment were grown from the ethanol-dichloromethane solution. The X-ray intensities for the  $CuL^{NEC}$  and  $CuL^{NEOB}$  complexes were collected with

an Oxford Sapphire CCD diffractometer using MoK $\alpha$  radiation  $\lambda = 0.71073 \text{ \AA}$ , at 293(2) K, by  $\omega$ -2 $\theta$  method. Structures were solved by direct methods and refined with the full-matrix least-squares method on  $F^2$  with the use of SHELX97 [65] program package. Analytical absorption corrections were applied (RED171 package of programs [66] Oxford Diffraction, 2000). No extinction correction was applied. Hydrogen atoms were located from the electron density maps and their positions were constrained in the refinement to keep the idealized geometry for aromatic CH, methylene and methyl groups, with the corresponding C-H distances of 0.97, 0.96 and 0.93  $\text{\AA}$ , as used in SHELXL-97 [65]). To keep the proper geometry, water molecules were restrained during the refinement with H-O and H-H distances of 0.84(1) and 1.4(1)  $\text{\AA}$ , respectively. In CuL<sup>NEC</sup>, the partial occupancy of 0.5 was set for the O4W water molecule, due to the large atomic displacement parameters (ADP) for O4W atom. On the other hand, for O1W the full occupancy was used, since it gave the better fit to the observed diffraction data. However, the large ADP for its O1W atom indicate the possible positional disorder of that water. In CuL<sup>NEOB</sup>, the void was found in the structure and the difference electron density map indicated the presence of the disordered ethanol molecule with the occupancy set to 0.25 based on the electron density level. Ethanol is disordered in such a way, that both its C31 and C31a atoms are common for two alternative positions, while the hydroxyl O32 occupies position of the methyl H atom in the alternative molecule. Therefore, total occupancy of C31 is 0.50 and results from the superposition of C31 and C31a from the molecule in the alternative position.

Magnetic susceptibility was measured from powder samples of solid material in the temperature range 2-300 K by using a SQUID susceptometer (Quantum Design MPMS-XL-5) in a magnetic field of 1000 Oe.

Voltammetric measurements were made with a computer controlled electrochemical system (ECO Chemie, Utrecht, The Netherlands) equipped with a PGSTA 30 model and driven by

GPES (ECO Chemie). A glassy carbon electrode with a surface area of  $0.035 \text{ cm}^2$  was used as a working electrode and a platinum wire served as the counter electrode. The reference electrode was an Ag wire as the quasi reference electrode. Ferrocene was added as an internal standard after completion of a set of experiments, and potentials are referenced vs. the ferrocenium/ferrocene couple ( $\text{Fc}^+/\text{Fc}$ ). Crystals of the  $\text{CuL}^{\text{NEC}}$  and  $\text{CuL}^{\text{NEOB}}$  complexes suitable for the X-ray diffraction experiment were obtained from the EtOH- $\text{CH}_2\text{Cl}_2$  solutions.

## 2.2. Preparations

### 2.2.1. Synthesis of Complexes

In a two-necked round-bottom flask, triethylamine (0.20 g, 2.00 mmol) was added to a solution of  $\text{H}_2\text{L}^{\text{NEX}}$  (1.00 mmol) in ethanol (50 ml).  $\text{Cu}(\text{OAc})_2 \cdot \text{H}_2\text{O}$  (0.2 g, 1.00 mmol) was added to this solution and the resulting mixture was refluxed for 2 h. Crystals suitable for X-ray diffraction were obtained by the slow evaporation of dichloromethane and ethanol mixture.

#### 2.2.1.1. Synthesis of $\text{CuL}^{\text{NEC}}$ Complex

Yield: 0.409 g (66%). Anal. Calcd. for  $\text{C}_{23}\text{H}_{25}\text{Cl}_4\text{CuN}_2\text{O}_4$  (499.722 g/mol). C, 40.1; H, 4.0; N, 4.9%. Found: C, 40.66; H, 4.05; N, 5.27%. IR (KBr,  $\text{cm}^{-1}$ ): 3445, 2896, 2354, 1633, 1452, 1317, 1170, 1029, 924, 865, 804, 748, 603, 447 UV-Vis in  $\text{CH}_2\text{Cl}_2$ :  $\lambda_{\text{max}}$ , nm ( $\epsilon$ ,  $\text{M}^{-1} \text{cm}^{-1}$ ): 432 (1277), 622 (723).

#### 2.2.1.2. Synthesis of $\text{CuL}^{\text{NEOB}}$ Complex

Yield: 0.426 g (65.5%). Anal. Calcd. for  $\text{C}_{33}\text{H}_{49}\text{CuN}_2\text{O}_6$  (534.2 g/mol). C, 61.8; H, 5.1; N, 4.8%. Found: C, 62.9; H, 5.24; N, 5.24%. IR (KBr,  $\text{cm}^{-1}$ ): 3445, 2937, 2356, 1616, 1459, 1423, 1310, 1269, 1201, 1060, 863, 808, 559, 511, UV-Vis in  $\text{CH}_2\text{Cl}_2$ :  $\lambda_{\text{max}}$ , nm ( $\epsilon$ ,  $\text{M}^{-1} \text{cm}^{-1}$ ): 437 (2026), 646 (1860).

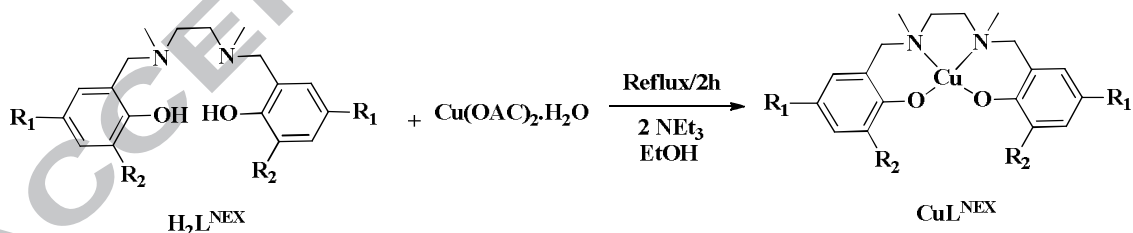
### 2.2.1.3. Catalytic activity of $\text{CuL}^{\text{NEOB}}$ complex in oxidation of alcohols

In a typical experiment, alcohol (1 mmol),  $\text{CuL}^{\text{NEOB}}$  (0.024 g, 5 mol%), TEMPO (0.024 g, 5 mol%) and  $\text{Cs}_2\text{CO}_3$  (0.650 g, 2 mmol) in 5 ml of oxygen saturated trifluorotoluene (TFT) were taken in a 15-mL two-necked round-bottom flask was equipped with oxygen balloon. The solution was magnetically stirred for some hours at room temperature and the mixture was filtered through a plug of silica, and then diluted with TFT (2 mL). The progress of the reaction was monitored by gas chromatography.

In a separate blank test, a 15-ml two-necked round-bottom flask was charged with the solution of copper(II) acetate, TEMPO or ligand in mixed medium of  $\text{Cs}_2\text{CO}_3$  (0.650 g, 2 mmol) in 5 ml of oxygen saturated TFT. Then the flask was equipped with an oxygen balloon at room temperature. The progress of the reaction was monitored by gas chromatography.

### 3. Results and Discussion

$\text{H}_2\text{L}^{\text{NEX}}$  [X: C and OB ], were prepared from N,N' dimethylethylenediamine, formaldehyde and 2,4-dichlorophenol or 2-tert-Butyl-4-methoxyphenol, in one step Mannich condensation. The copper(II) complexes were synthesized by the following procedure (Scheme 5).



**Scheme 5.** The reaction pathway for the synthesis of  $\text{CuL}^{\text{NEX}}$

In IR spectra of complexes, replacement of the strong and sharp  $\nu_{\text{OH}}$  stretch band of the phenols around  $3300\text{-}3500 \text{ cm}^{-1}$  by a broad band, proved the coordination of phenol groups to the metal.

In both complexes, the absorption maxima observed in the near-UV regions (below 300 nm) are attributed to  $\pi \rightarrow \pi^*$  transitions of phenolate units. There are two absorption features in the visible spectrum of  $\text{CuL}^{\text{NEX}}$  complexes which are assigned to phenolate ( $\pi$ ) -to- Cu(II) ( $d\pi^*$ ) charge transfer (LMCT) transitions (Fig.1, Table 1). It was observed that, when OMe electron donating substituents are placed on the phenolate groups, the position of LMCT bands shifted to higher wavelengths (lower energy).

Figure 1

Table 1.  $\lambda_{\text{max}}/\text{nm}$  ( $\epsilon/\text{M}^{-1}\text{cm}^{-1}$ ) LMCT band of complexes  $\text{CuL}^{\text{NEX}}$  (X: C, B and OB)

$\text{CuL}^{\text{NEX}}$	$\lambda_{\text{max}}/\text{nm}(\epsilon/\text{M}^{-1}\text{cm}^{-1})$	$\lambda_{\text{max}}/\text{nm}(\epsilon/\text{M}^{-1}\text{cm}^{-1})$
$\text{CuL}^{\text{NEC}}$	431 (1268)	625 (715)
$\text{CuL}^{\text{NEOB}}$	460 (2285)	665 (1864)

### 3.1. Single crystal data collection and the crystal structure description

Crystal and refinement data for the  $\text{CuL}^{\text{NEC}}$  and  $\text{CuL}^{\text{NEOB}}$  are summarized in Table 2.

Selected bond lengths and angles are given in Tables 3.

Table 2. Crystal data and structure refinement for  $\text{CuL}^{\text{NEC}}$  and  $\text{CuL}^{\text{NEOB}}$ 

Identification code	$\text{CuL}^{\text{NEC}}$	$\text{CuL}^{\text{NEOB}}$
Empirical formula	$\text{C}_{18}\text{H}_{21.5}\text{Cl}_4\text{CuN}_2\text{O}_{3.75}$	$\text{C}_{28.5}\text{H}_{43.5}\text{CuN}_2\text{O}_{4.25}$
Formula weight	531.21	545.69
Temperature; K	293(2)	293(2)
Wavelength; Å	0.71073	0.71073
Crystal system, space group	Orthorhombic, Pca2(1)	Triclinic, P-1
Unit cell dimensions; Å	a = 22.7101(6)	a = 10.7996(6)
	b = 12.3188(3)	b = 11.3898(10)
	c = 16.0313(5)	c = 13.1074(9)
		$\alpha = 98.658(7)$
		$\beta = 109.474(6)$
		$\gamma = 95.963(6)$
Volume; Å <sup>3</sup>	4484.9(2)	1482.06(19)
Z, Calculated density; Mg/m <sup>3</sup>	8, 1.573	2, 1.223
Absorption coefficient; mm <sup>-1</sup>	1.476	0.771
F(000)	2164	583
Crystal size; mm	0.29 x 0.15 x 0.02	0.77 x 0.43 x 0.19
Theta range for data collection, °	2.20 to 28.14	2.23 to 28.03
Limiting indices	-22 ≤ h ≤ 29, -15 ≤ k ≤ 16,	-14 ≤ h ≤ 14, -14 ≤ k ≤ 14,

	-20<=l<=17	-16<=l<=17
Reflections collected / unique	27516 / 9427 R(int)=0.0841	9250 / 6257 R(int)=0.0460
Completeness to $\theta = 25.00$	99.9 %	99.9 %
Absorption correction	Analytical	Analytical
Max. and min. transmission	0.9663 and 0.6766	0.8665 and 0.5891
Refinement method	Full-matrix least-squares on $F^2$	Full-matrix least-squares on $F^2$
Data / restraints / parameters	9427 / 1 / 523	6256 / 3 / 334
Goodness-of-fit on $F^2$	0.838	1.045
Final R indices [ $I > 2\sigma(I)$ ]	R1=0.0534, wR2=0.1029	R1=0.0536, wR2=0.1382
R indices (all data)	R1=0.1309, wR2=0.1181	R1=0.0723, wR2=0.1534
Absolute structure parameter	0.308(17)	
Largest diff. peak and hole; $e.\text{\AA}^{-3}$	0.685 and -0.401	0.807 and -0.766

**Table 3.** Selected bond lengths [ $\text{\AA}$ ] and angles [ $^\circ$ ] for  $\text{CuL}^{\text{NEC}}$  and  $\text{CuL}^{\text{NEOB}}$

$\text{CuL}^{\text{NEC}}$	Molecule1	$\text{CuL}^{\text{NEC}}$	Molecule2	$\text{CuL}^{\text{NEOB}}$	
Cu1-O1	1.930(5)	Cu2-O21	1.923(5)	Cu1-O1	1.884(2)
Cu1-O2	1.952(5)	Cu2-O22	1.906(5)	Cu1-O2	1.889(2)
Cu1-N1	2.026(6)	Cu2-N21	2.004(6)	Cu1-N1	2.042(2)
Cu1-N2	2.056(6)	Cu2-N22	2.062(6)	Cu1-N2	2.026(3)
Cu1-O2W	2.385(6)	Cu2-O3W	2.550(5)		
angles [deg]					
O1-Cu1-O2	89.7(2)	O22-Cu2-O21	89.6(2)	O1-Cu1-O2	90.15(9)
O1-Cu1-N1	89.9(2)	O21-Cu2-N21	92.9(3)	O1-Cu1-N1	93.51(10)
O2-Cu1-N1	169.4(2)	O22-Cu2-N21	174.0(3)	O2-Cu1-N1	168.84(10)
O1-Cu1-N2	170.2(2)	O21-Cu2-N22	172.3(3)	O1-Cu1-N2	167.50(10)
O2-Cu1-N2	92.1(2)	O22-Cu2-N22	90.8(2)	O2-Cu1-N2	92.50(9)
N1-Cu1-N2	86.5(2)	N21-Cu2-N22	86.0(3)	N2-Cu1-N1	86.19(11)
O1-Cu1-O2W	93.2(2)	O3W-Cu2-O21	93.9(2)		
O2-Cu1-O2W	98.6(2)	O3W-Cu2-O22	91.6(2)		
N1-Cu1-O2W	92.0(2)	O3W-Cu2-N21	93.7(2)		
N2-Cu1-O2W	96.0(2)	O3W-Cu2-N22	93.8(2)		

### 3.1.1. X-ray Crystal Structure of $\text{CuL}^{\text{NEC}}$

The complex crystallizes in the orthorhombic space group  $Pca2_1$ . The asymmetric unit contains one molecule of the  $[\text{CuL}^{\text{NEC}}(\text{H}_2\text{O})]$  complex, second molecule  $\text{CuL}^{\text{NEC}}$  with weakly interacting water and two other water molecules. The complex molecules are positioned in the crystal lattice with the equatorial  $\text{CuN}_2\text{O}_2$  moieties almost parallel (dihedral angle  $5.0(3)^\circ$ ) but axial water ligands pointing to the opposite directions (Figure. 2).

**Figure 2**

In the first molecule, the coordination sphere  $\text{CuN}_2\text{O}_3$  has the square pyramid geometry with the axially bound O2W water molecule. The Cu1-O1 and Cu1-O2 distances are approximately 0.1 Å shorter than the Cu-N distances (Table 3). The axial Cu1-O2W bond of 2.385(6) Å is significantly longer than bonds found in the equatorial  $\text{CuN}_2\text{O}_2$  plane. The bond angles in the base of the coordination pyramid reveal the largest deviations from the square geometry as indicated by the O-Cu1-N angles involving atoms positioned trans. The angles between the axial Cu1-O2W and bonds formed within the square plane vary from N1-Cu1-O2W 92.0(2) ° to O2-Cu1-O2W 98.6(2)°.

In the second molecule, the axial interaction Cu2-O3W is significantly longer than in the first molecule, with the distance Cu2-O3W of 2.550(5) Å. The weaker interaction to that ligand seems to result in the shortening of the Cu2-O22 and Cu2-N21 bond distances within the square-planar coordination sphere of Cu2 (Table 3), up to 0.046 Å, compared to those found in the first molecule. Binding of the axial water molecules is structurally similar to the weak coordination of the axial Tyr495 residue in the GOase [4] (Scheme 2). In molecule 2 the largest deformation from the square geometry are found for the angles formed by equatorial donor atoms positioned trans to each other. The angles N/O-Cu2-O3W in molecule 2 are closer to 90 °, than those found in molecule 1, what might be related to the repulsions within the coordination sphere of Cu1 with the shorter axial Cu-O bond but also to the intramolecular strain caused by the differences in the ligand conformation. These differences between two complex molecules are emphasized by the deviation of central Cu ion from the equatorial best  $\text{N}_2\text{O}_2$  plane towards the axial water, being 0.176(3) and 0.111(3) Å for Cu1 and Cu2, respectively.

The valence geometry of the  $\text{H}_2\text{L}^{\text{NEC}}$  ligands is typical for such systems. The equatorial arrangement of the  $\text{H}_2\text{L}^{\text{NEC}}$  ligand in the coordination sphere results in the twist of the central ethylenediamine moiety, with the torsion angle N1-C8-C9-N2 being -55.1(9)°, a value typical

for analogous Fe or Mn complexes [64, 67]. In molecule 2 the corresponding N21-C28-C29-N22 torsion angle is  $-21.8(19)^\circ$ , what further emphasizes the differences within the coordination sphere of Cu ions. As a result, the methyl groups bound to N in molecule 1 are positioned trans, while in molecule 2 are cis relative to each other (Figure 2). The dihedral angles between the phenolic rings of the  $L^{\text{NEC}}$  ligands are  $30.3^\circ$  and  $2.0^\circ$ .

In molecule 1, the central chelate ring Cu1-N1-C8-C9-N2 has a conformation twisted on C8-C9, the Cu1-O1-C1-C6-C7-N1 is an envelope on N1, while Cu1-O2-C16-C11-C10-N2 is an envelope on C10. In molecule 2, the corresponding rings are envelopes on N21, N22 and C27.

Analysis of the crystal packing revealed the series of H-bonds involving water OH as donors and  $L^{\text{NEC}}$  ligands Cl substituents and O atoms as acceptors (Table 4S, Supporting Information).

### 3.1.2. X-ray Crystal Structure of $\text{CuL}^{\text{NEOB}}$

The complex crystallizes in the triclinic space group P-1. The asymmetric part of the reported structure consists of the complex molecule  $\text{CuL}^{\text{NEOB}}$  and a disordered ethanol molecule (Figure 3). The absolute configuration R,R is found on N1, N2 atoms of the molecule in the asymmetric unit. However, the centrosymmetric space group P-1 results in the equimolar presence of S,S-N1,N2 isomer in the structure. The coordination sphere  $\text{CuN}_2\text{O}_2$  has a square planar geometry with pairs of N and O atoms occupying cis positions due to the tetradentate coordination of the  $L^{\text{NEOB}}$  ligand. The Cu1-O1 and Cu1-O2 distances of 1.882(2) and 1.889(2) Å, respectively, are significantly shorter than those found for  $\text{CuL}^{\text{NEC}}$  complex. On the other hand, the Cu-N distances in  $\text{CuL}^{\text{NEOB}}$  are similar to those found for molecule 1 of  $\text{CuL}^{\text{NEC}}$ , but reveal statistically significant differences when compared to molecule 2 of  $\text{CuL}^{\text{NEC}}$  (Table 3). Such geometry seems to result from the NEOB ligand conformation described with the torsion angle N1-C8-C9-N2  $-54.0(5)^\circ$ , similar to that of  $\text{CuL}^{\text{NEC}}$  molecule

1 or analogous Fe and Mn complexes [64, 67]. The largest angular deformation from the square geometry is found for O1-Cu1-N2 of 167.5(1) °. Deviation of Cu1 from the N<sub>2</sub>O<sub>2</sub> best plane is 0.010(2) Å.

### Figure 3

The extended molecular conformation of L<sup>NEOB</sup> is found, with the dihedral angle between best planes of the phenolic being 32.28(17) °. Three chelate rings are formed by L<sup>NEOB</sup> ligand. Ring Cu1-N1-C8-C9-N2 is twisted on C8-C9, while both six-membered Cu1-O1-C1-C6-C7-N1 and Cu1-O2-C16-C11-C10-N2 have a screw-boat conformation.

The valence geometry of the L<sup>NEOB</sup> ligands is typical for such systems. Due to the syn-clinal conformation of the central ethylenediamine moiety of L<sup>NEOB</sup>, the N-Met groups are positioned trans relative to each other, similar to the orientation found in Molecule 1 of CuL<sup>NEC</sup>. The OMe groups of L<sup>NEOB</sup> ligand are nearly co-planar with the phenolic rings, with torsion angles C5-C4-O3-C21 -2.7(6) ° and C12-C13-O4-C24 10.9(6) °.

The hydroxyl group of ethanol participates in the H-bond with O3[-x,-y,-z], with the O...O distance being 2.900(4) Å. Analysis of the intermolecular interactions revealed the C-H... $\pi$  interactions between C22 and C23 methyl groups and the being C22-H22B...Cg(C11...C16)[-x,1-y,-z] 2.91 and C22-H22C...Cg(C11...C16)[-x,1-y,-z] 2.97 Å, C23-H23A...Cg(C1...C6) [-x,2-y,-z] of 2.80 Å.

### 3.2. Magnetic susceptibility measurement

Temperature variation of measured susceptibility  $\chi(T)$  for CuL<sup>NEC</sup> and CuL<sup>NEOB</sup> is shown in Fig 4. The presented data were corrected for the temperature-independent Larmor diamagnetic susceptibility obtained from Pascal's tables [68] and for the sample holder contribution. The susceptibility of both samples increases with decreasing temperature, following a Curie 1/ T law, which indicates paramagnetic behavior. Paramagnetic behavior is

also confirmed from the temperature independent effective magnetic moment of both complexes (inset in Fig. 4). The effective magnetic moments of both complexes lie between 1.70 and 1.80 BM for temperatures above 5 K. The values are slightly smaller than the spin-only value of  $\mu_{\text{eff}} = 1.9$  BM for the isolated Cu(II) ion ( $S = 1/2$ ) [69], but very close to the values measured in other copper complexes (reported values in [70] were 1.77–1.83 BM). This confirms the presence of one unpaired electron in the copper center of both complexes. A very small downturn of the measured effective moment of  $\text{CuL}^{\text{NEC}}$  at temperatures below 5 K could be attributed to a very weak antiferromagnetic interaction between the copper monomers. This was confirmed by applying a Curie–Weiss law  $\chi = C/(T-\theta)$  to fit the data above 20 K. The obtained Curie–Weiss temperature was  $\theta = -0.14$  K (Table 4).

**Figure 4**

**Table 4.** Calculated parameters  $C$  and  $\theta$  from the fit of the measured data. The effective magnetic moment  $\mu_{\text{eff}}$  per iron ion was calculated using a relation

	$C$ (emu K/mol)	$\theta$ (K)	$\mu_{\text{eff}}$ (BM)
$\text{CuL}^{\text{NEC}}$	0.403	0.380	1.8
$\text{CuL}^{\text{NEOB}}$	0.366	0.033	1.72

**Table 4**

### 3.3. Electrochemistry

Cyclic voltammogram (CV) of complexes have been recorded in  $\text{CH}_2\text{Cl}_2$  solutions containing 0.1 M  $[(n\text{-Bu})_4\text{N}]\text{ClO}_4$  as a supporting electrolyte.

This research reveals that there are two quasi-reversible oxidation peaks for  $\text{CuL}^{\text{NEOB}}$  complex in the positive potential range and there is one irreversible oxidation peaks for  $\text{CuL}^{\text{NEC}}$  complex. As the further oxidation of copper (II) redox process occurs at higher redox potentials, these redox processes are probably attributed to the ligand centered redox

processes in which phenolate group yields phenoxyl radical in the complex, but there is no direct evidence available yet. This observation can be attributed to the shielding effect of *t*-Bu groups for stabilization of phenoxyl radical groups. Typical cyclic voltammogram (CV) of  $\text{CuL}^{\text{NEOB}}$ , is presented in Figure 5.

**Figure 5**

cyclic voltammogram (CV) of  $\text{CuL}^{\text{NEC}}$ , is presented in Figure 1S. The metal-centred voltammograms have been observed in the negative potential range, what corresponds to the  $\text{Cu}^{\text{II}}/\text{Cu}^{\text{I}}$  reduction of copper complexes. These metal-centered voltammograms are electrochemically irreversible for  $\text{CuL}^{\text{NEC}}$  complex and quasi-reversible for  $\text{CuL}^{\text{NEOB}}$  complexes.

### 3.4. EPR spectroscopy results

Frozen solution EPR shows a single isotropic signal with a *g* value of 2.045 and 2.064 more than the free electron *g* value attributed to single-electron copper (II)  $d^9$  configuration. A typical EPR spectrum of  $\text{CuL}^{\text{NEOB}}$  has been shown in Figure 6. EPR of  $\text{CuL}^{\text{NEC}}$  has been shown in Figure 2S.

**Figure 6**

### 3.5. The catalytic activity of $\text{CuL}^{\text{NEX}}$ complex in the aerobic oxidation of alcohols

In continuation of our studies on the application of  $\text{CuL}^{\text{NEX}}$  complexes, we report on the aerobic oxidation of alcohols to corresponding aldehydes using this complex. To study the catalytic oxidation of alcohols mediated by  $\text{CuL}^{\text{NEX}}$ , benzyl alcohol was chosen as a model compound and the reaction conditions were optimized accordingly. Our experiments showed that among the employed complexes,  $\text{CuL}^{\text{NEC}}$  exhibited superior catalytic

performance than  $\text{CuL}^{\text{NEOB}}$  (50% conversion) in catalyzing aerobic oxidation of benzyl alcohol to benzaldehyde. This is most likely owed to the fact that the electron withdrawing substituents at phenolate groups provided different electron densities on the Cu center in this complex and should yield higher conversions of benzyl alcohol. Alternatively, time screening of the  $\text{CuL}^{\text{NEX}}/\text{TEMPO}$  system alcohol oxidation showed the same initiation time for both complexes (Fig. 7). It considers that  $\text{CuL}^{\text{NEOB}}$  shows lower activity during the reaction time. In addition after around 2 hrs a higher decrease in the rate of reactivity for  $\text{CuL}^{\text{NEOB}}$  was observed. It can possibly attributed to the lower stability of this complex during the reaction time.

#### Figure 7

Next, we investigated the effect of bases for oxidation of benzyl alcohol. Using bases such as KOH and  $\text{NaHCO}_3$ , the alcohol conversions were lower than that for  $\text{Cs}_2\text{CO}_3$  (Table 6, entries 3-5). In the next stage, the amount of  $\text{Cs}_2\text{CO}_3$  was also optimized (Table 5, entries 1, 2) and the best result was achieved when 2 equivalents of  $\text{Cs}_2\text{CO}_3$  were used.

The solvent effect was also investigated and the results have been summarized in Table 7. In this context, various organic solvents such as  $\text{CH}_3\text{CN}$ ,  $\text{CH}_2\text{Cl}_2$  etc. were studied and TFT appeared to be the most favorable solvent for the described transformation (52%, Table 6, entries 1).

**Table 5.** The effect of base on the alcohol oxidation

Entry	Base	CuL <sup>NEC</sup>	
		Time (h)	Conversion (%)
<b>1</b>	4 mmol Cs <sub>2</sub> CO <sub>3</sub>	6	<b>58</b>
<b>2</b>	<b>2 mmol Cs<sub>2</sub>CO<sub>3</sub></b>	<b>6</b>	<b>52</b>
<b>3</b>	4 mmol NaHCO <sub>3</sub>	12	25
<b>4</b>	2 mmol NaHCO <sub>3</sub>	12	20
<b>5</b>	2 mmol NaNO <sub>3</sub>	8	10
<b>6</b>	4 mmol KOH	8	9

**Table 6.** The effect of solvent on the alcohol oxidation

Entry	Solvent	Time (h)	Conversion (%)
<b>1</b>	<b>TFT</b>	<b>6</b>	<b>52</b>
<b>2</b>	Toluene	8	29
<b>3</b>	CH <sub>3</sub> CN	6	9
<b>4</b>	CH <sub>2</sub> Cl <sub>2</sub> +TFT	6	6
<b>5</b>	TFT+CH <sub>3</sub> COOH	6	5

The effect of catalyst loading between 5.0 to 15.0 mol% was also studied within 12 hrs. (Table 7) and it was revealed that the maximum yield of benzaldehyde was obtained when 15.0 mol% of  $\text{CuL}^{\text{NEC}}$  were employed. In addition, when the reaction condition employed for catalytic experiment are 15.0 mol% of  $\text{CuL}^{\text{NEC}}$ , the impact of TEMPO loading was then studied between 5-10 mol% under otherwise the same reaction condition indicated in Table 7. The best result was obtained when the amount of TEMPO was chosen 5 mol% (Table 8). The blank tests verified “ligand-free”, copper(II) acetate/ $\text{Cs}_2\text{CO}_3$  affords aldehyde in low yield (Table 9). Supposing the effect of the ligand on increasing the alcohol conversion, the blank test with copper(II) acetate/ $\text{Cs}_2\text{CO}_3$  and free ligand improved the aldehyde yield. Comparing these results with the same for  $[\text{CuL}^{\text{NEC}}-\text{Cs}_2\text{CO}_3]$  as catalyst system lead us to this fact that the structure of this coordination copper complex and metal-ligand synergistic effects have an important role in the oxidation of alcohols.

**Table 7.** The effect of  $\text{CuL}^{\text{NEC}}$  equivalences on the alcohol oxidation

Entry	$\text{CuL}^{\text{NEC}}$ (mol%)	Time (h)	Conversion (%)
1	15	12	99.5
2	12	12	91
3	10	12	82
4	5	12	70
5	8	12	20

**Table 8.** The effect of TEMPO equivalences on the alcohol oxidation

Entry	TEMPO (mmol)	Time (h)	Conversion (%)
1	0.25	10	61
2	0.05	6	60
3	0.5	6	27
4	1	10	16

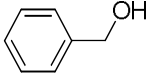
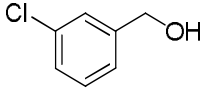
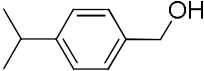
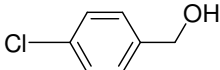
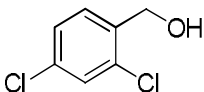
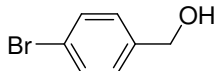
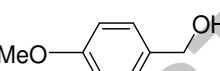
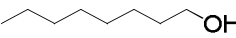
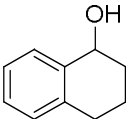
**Table 9.** The result of blank test for oxidation of benzyl alcohol with catalyst system

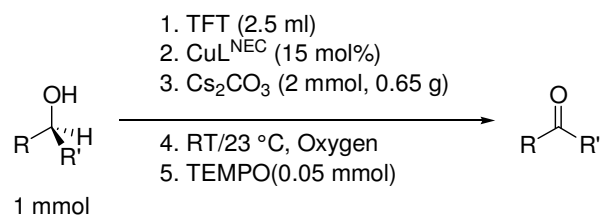
Entry	Catalytic system	Time (h)	Conversion (%)
1	Copper(II) acetate /Cs <sub>2</sub> CO <sub>3</sub>	12	24
2	H <sub>2</sub> L <sup>NEC</sup> /Cs <sub>2</sub> CO <sub>3</sub>	12	35
3	Copper(II) acetate /Cs <sub>2</sub> CO <sub>3</sub> / H <sub>2</sub> L <sup>NEC</sup>	12	50
4	CuL <sup>NEC</sup> /Cs <sub>2</sub> CO <sub>3</sub>	12	72

To assess the general scope of the catalytic oxidation, several types of benzylic, and other, different kinds of alcohols were chosen as substrates. Under optimized reaction conditions (TFT using 15 mol% of CuL<sup>NEC</sup>, 2 mmol Cs<sub>2</sub>CO<sub>3</sub> and 0.05 mmol TEMPO), various substituted benzaldehydes were obtained from their corresponding, readily available, alcohols. According to the literature [71-73], in the “copper complex-Cs<sub>2</sub>CO<sub>3</sub>” the higher activity in TFT may be attributed to the possible adduct formation between copper and/or cesium cations and aromatic solvent as well as to the polarity effect and higher solubility of

O<sub>2</sub> in this fluorinated solvent. These results led us to suggest that Cs<sub>2</sub>CO<sub>3</sub> most likely acts not only as a strong base for deprotonating of alcohol but also as a heterogeneous support for CuL<sup>NEC</sup> to produce an stable CuL<sup>NEC</sup>-Cs<sub>2</sub>CO<sub>3</sub> catalytic species [74-76]. In this system, CuL<sup>NEC</sup> is slightly soluble in TFT while Cs<sub>2</sub>CO<sub>3</sub> is not soluble. Therefore, CuL<sup>NEC</sup>-Cs<sub>2</sub>CO<sub>3</sub> catalyst can be possibly considered as an actual intermediate between homogenous and heterogeneous catalyst. The results for oxidations of variety of benzyl alcohols are summarized in Table 10. Our studies show that CuL<sup>NEC</sup> is selective towards benzyl alcohol while is totally inactive for aliphatic alcohols (Table 10). As can be seen, unsubstituted benzylic alcohol is oxidized more efficiently than substituted ones (Table 10). These results suggest that the influence of the substituent appears to be related to both electronic and steric effects. This catalyst doesn't show any activity against secondary alcohols. The catalytic activity of CuL<sup>NEC</sup> complex in the aerobic oxidation of alcohols is shown in Schemes 5 and 6. The results of this study show that the carbonyl compound is the only product obtained with comparatively good yields. Generally, over-oxidation of the primary alcohols to the corresponding acids occurs with other catalysts, but in the present work the formation of acids was not observed (Scheme 6).

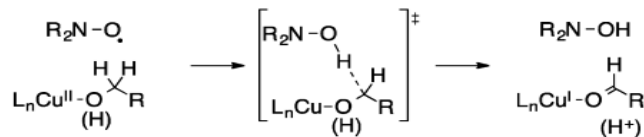
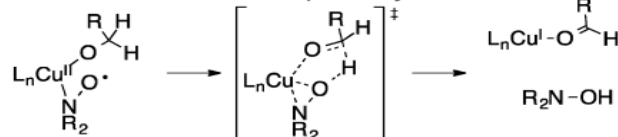
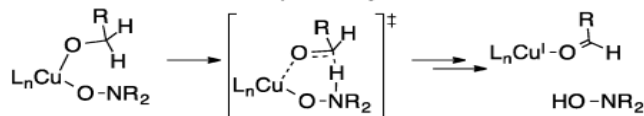
**Table 10.** Alcohol oxidation results in TFT, catalysed by Copper [CuL<sup>NEC</sup>] and TEMPO in a presence of Cs<sub>2</sub>CO<sub>3</sub> as base and O<sub>2</sub> as oxidant

Entry	Substrate	Time (h)	Conversion (%)	Time (h)	Conversion (%)
1		12	100	24	100
2		8	92	12	99
3		12	91	24	96
4		8	93	12	96
5		12	84	24	92
6		12	75	24	91
7		12	73	24	89
8		12	64	24	84
9		12	79	24	80
10		12	16	24	24
11		12	9	24	10
12		8	4	12	5

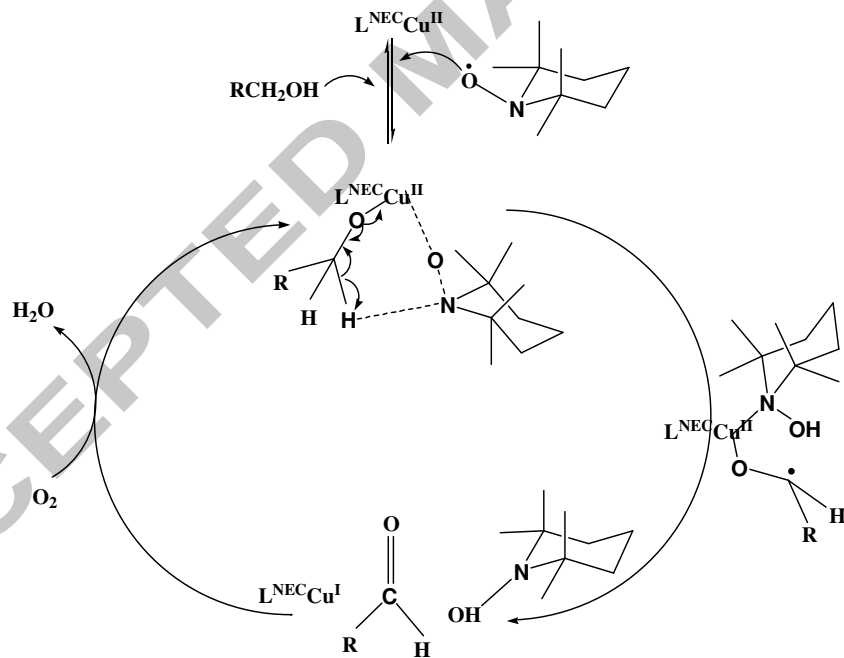


**Scheme 6.** Catalytic activity of CuL<sup>NEC</sup> in the aerobic oxidation of alcohols.

Since CuL<sup>NEC</sup> is not effective in the absence of additional base, we suggest that Cs<sub>2</sub>CO<sub>3</sub> is responsible for the deprotonation of alcohols. Coordination of this alcoholate to copper(II) complex produces an alkoxide complex. Intermolecular abstraction of hydrogen with TEMPO leads to the formation of ketyl radical. In other word, nitroxyl radicals act as redox-active organic co-catalyst to facilitate the 1 H<sup>+</sup>/2e<sup>-</sup> process associated with conversion of an alkoxide ligand to a carbonyl compound. Stoichiometric reactivity studies showed that both copper(II) and TEMPO participate in the alcohol oxidation step [62]. It suggest that an electron transfer to copper produces aldehyde and Cu(I) species. and aerobic oxidation of Cu(I) and TEMPO-H affords Cu(II) and TEMPO species back to the original Cu(II) complex and cocatalyst. Based on Stahl studies, there are three different mechanisms for oxidation of the alkoxide ligand (Scheme 7): bimolecular H-atom transfer, H-atom transfer to an η<sup>2</sup>-nitroxyl ligand, and hydrogen transfer to an η<sup>1</sup>-nitroxyl ligand. Stahl group have reported that the last exhibits the lowest-energy pathway for alcohol oxidation, rationalizes the observed selectivity for primary over secondary alcohol oxidation (Scheme 7) [62].

**A. Bimolecular Hydrogen-Atom Transfer****B. H-Atom Transfer to an  $\eta^2$ -Nitroxyl****C. H-Atom Transfer to an  $\eta^1$ -Nitroxyl****Scheme 7.** Stahl mechanistic Proposals for Cu<sup>II</sup>/Nitroxyl mediated alcohol oxidation [62]

Considering experimental results and results of studies reported previously, our proposed reaction mechanism for the system is shown in scheme 8.

**Scheme 8.** The possible reaction pathway in the catalytic cycle of alcohol oxidation using CuL<sup>NEC</sup>/TEMPO/Cs<sub>2</sub>CO<sub>3</sub> catalytic system**4. Conclusion**

In summary, two new copper(II) complexes ( $\text{CuL}^{\text{NEOB}}$  and  $\text{CuL}^{\text{NEC}}$ ) of aminophenol-based ligands were synthesized and characterized.

Electrochemical oxidation of these complexes yielded the corresponding Cu(II)-phenoxy radical species.

In addition, highly efficient, and eco-friendly TEMPO-mediated oxidation of alcohol to aldehyde was achieved with molecular oxygen as oxidant and non-precious catalyst  $\text{CuL}^{\text{NEC}}$ - $\text{Cs}_2\text{CO}_3$  system. In conclusion, this system is found to be very efficient for a wide range of benzylic alcohols. Advantages of this catalytic system are the use of low price copper catalyst, molecular oxygen, high selectivity, low loading of TEMPO under mild reaction conditions (room temperature). The disadvantage of the system is the lack of activity against aliphatic primary and secondary alcohols and high loading of copper complex.

**Appendix A.** The structural data for  $\text{CuL}^{\text{NEC}}$  and  $\text{CuL}^{\text{NEOB}}$  have been deposited with the Cambridge Crystallographic Data Centre, the deposition number being CCDC 1041129 and 1041130 respectively. <http://www.ccdc.cam.ac.uk/conts/retrieving.html>, or from the Cambridge Crystallographic Data Centre, 12 Union Road, Cambridge CB2 1EZ, UK; fax: (+44) 1223-336-033; or e-mail: [deposit@ccdc.cam.ac.uk](mailto:deposit@ccdc.cam.ac.uk).

### Acknowledgments

Authors are grateful to the Institute for Advanced Studies in Basic Sciences (IASBS), Ljubljana, Changwon and Nicolaus Copernicus Universities for their valuable help. E. Safaei gratefully acknowledges the support by the Institute for Advanced Studies in Basic Sciences (IASBS) Research Council under Grant No. G2014IASBS127. Yong-Il Lee acknowledges support by the Priority Research Centers Program (NRF 2010-0029634) through the National Research Foundation of Korea (NRF).

**References**

- [1] R. Horton, L.A. Moran, G. Scrimgeour, M. Perry, D. Rawn, Principles of Biochemistry 4th Edition, Pearson Education (US) (2005) pp 40-55.
- [2] W. Becker, L.J. Kleinsmith, J. Hardin, G.P. Bertoni, The World of the Cell, San Francisco: Benjamin Cummings (2008) 45-52.
- [3] L. Jr. Que, W. B. Tolman, Nature 455 (2008) 333-340.
- [4] L. Xie, PNAS 98 (2001) 12863-12865.
- [5] F. Thomas, Eur. J. Inorg. Chem. (2007) 2379-2404.
- [6] N. Ito, S. E. V. Phillips, C. Stevens, Z. B. Ogel, M. J. McPherson, J. N. Keen, K. D. S. Yadav, P. F. Knowles, Nature, 350 (1991) 87-90.
- [7] N. Ito, S. E. V. Phillips, K. D. S. Yadav, P. F. Knowles, J. Mol. Biol. 238 (1994), 794-814.

- [8] F. Michel, F. Thomas, S. Hamman, C. Philouze, E. Saint-Aman, J. L. Pierre, *Eur. J. Inorg. Chem.* (2006) 3684-3696.
- [9] M.M. Whittaker, J.W. Whittaker, *J. Biol. Chem.* 265 (1990) 9610-9613.
- [10] A. Harriman, *J. Phys. Chem.* 91 (1987) 6102-6104.
- [11] A. Boussac, A.L. Eteinne, *Biochim. Biophys. Acta* 766 (1984) 576-581.
- [12] W. Tagaki, in: S. Oae (Ed.), *Organic Chemistry of Sulfur*, Plenum Press, New York, (1977) pp 231-302.
- [13] A. Mijovilovich, S. Hamman, F. Thomas, F. M. F. de Groot, B.M. Weckhuysen *Phys. Chem. Chem. Phys.* 13 (2011) 5600-5604.
- [14] M. A. A. Khalid, *Electrochemistry* (2013) pp 40-60.
- [15] M. M. Whittaker, Y. Y. Chuang, J.W. Whittaker, *J. Am. Chem. Soc.* 115 (1993) 10029-10035.
- [16] S. Itoh, K. Hirano, A. Furuta, M. Komatsu, Y. Ohshiro, A. Ishida, S. Takamuku, T. Kohzuma, N. Nakamura, S. Suzuki, *Chem. Lett.* (1993) 2099-2102.
- [17] S. Itoh, S. Takayama, R. Arakawa, A. Furuta, M. Komatsu, A. Ishida, S. Takamuku, S. Fukuzumi, *Inorg. Chem.* 36 (1997) 1407-1416.
- [18] S. Oae, M. Yoshihara, W. Tagaki, *Bull. Chem. Soc. Jpn.* 40 (1967) 951-953.
- [19] G.N.R. Tripathi, R.H. Schuler, *J. Phys. Chem.* 92 (1988) 5129-5133.
- [20] R.A. Sheldon, J.K. Kochi, *Metal-Catalyzed Oxidation of Organic Compounds*, Academic Press, New York, (1991) 25-60.
- [21] S.V. Ley, J. Norman, W. P. Griffith, S.P. Marsden, *Synthesis* 7 (1994) 639-666.
- [22] M. Hudlicky, *Oxidations in Organic Chemistry*, ACS, Washington, DC, (1990) pp 65-78.
- [23] C. Jallabert, H. Riviere, *Tetrahedron Lett.* 14 (1977) 1215-1218.
- [24] P. Capdeville, P. Audebert, M. Maumy, *Tetrahedron Lett.* 25 (1984) 4397-4400.

- [25] J. A. Halfen, V.G. Jr. Young, B. W. Tolman, *Angew. Chem., Int. Ed.* 35 (1996) 1687-1690.
- [26] J. A. Halfen, B. A. Jazdzewski, S. Mahapatra, L. M. Berreau, E. C. Wilkinson, L. Jr. Que, W. B. Tolman, *J. Am. Chem. Soc.* 119 (1997) 8217-8227.
- [27] A. Sokolowski, H. Leutbecher, T. Weyhermuller, R. Schnepf, E. Bothe, E. Bill, P. Hildebrandt, K. Wieghardt, *JBIC, J. Biol. Inorg. Chem.* 2 (1997) 444-453.
- [28] J. Muller, T. Weyhermuller, E. Bill, P. Hildebrandt, L. Ould- Moussa, T. Glaser, K. Wieghardt, *Angew. Chem. Int. Ed.* 37 (1998) 616-619.
- [29] S. Bhaduri, N. Y. Sapre, *J. Chem. Soc., Dalton Trans.* 12 (1981) 2585-2586.
- [30] N. Kitajima, K. Whang, Y. Morooka, A. Uchida, Y. Sasada, *J. Chem. Soc., Chem. Commun.* 20 (1986) 1504-1505.
- [31] Y. Wang, T. D. P. Stack, *J. Am. Chem. Soc.* 118 (1996) 13097-13098.
- [32] Y. Wang, J. L. DuBois, B. Hedman, K. O. Hodgson, T. D. Stack, *Science* 279 (1998) 537-540.
- [33] E. Saint-Aman, S. Menage, J. L. Pierre, E. Defrancq, G. Gellon, *New J. Chem.* (1998) 393-397.
- [34] S. Velusamy, T. Punniyamurthy, *Eur. J. Org. Chem.* 20 (2003) 3913-3915.
- [35] P. Chaudhuri, M. Hess, U. Florke, K. Wieghardt, *Angew. Chem. Int. Ed.* 37 (1998) 2217-2220.
- [36] P. Chaudhuri, M. Hess, T. Wehermuller, K. Wieghardt, *Angew. Chem. Int. Ed.* 38 (1999) 1095-1097.
- [37] T. K. Paine, T. Weyhermuller, K. Wieghardt, P. Chaudhuri, *Dalton Trans.* (2004) 2092-2101.
- [38] P. Chaudhuri, M. Hess, J. Mueller, K. Hildenbrand, E. Bill, T. Weyhermueller, K. Wieghardt, *J. Am. Chem. Soc.* 121 (1999) 9599-9610.

- [39] R. J. M. K. Gebbink, T.D. Stack, *J. Inorg. Biochem.* 74 (1999) 138-140.
- [40] F. Thomas, G. Gellon, I. Gautier-Luneau, E. Saint-Aman, J. L. Pierre, *Angew. Chem., Int. Ed.* 41 (2002) 3047-3050.
- [41] S. Velusamy, A. Srinivasan, T. Punniyamurthy, *Tetrahedron Lett.* 47 (2006) 923-926.
- [42] P. Chaudhuri, M. Hess, J. Mueller, K. Hildenbrand, E. Bill, T. Weyhermueller, K. Wieghardt, *J. Am. Chem. Soc.* 121 (1999) 9599-9616.
- [43] R. J. M. K. Gebbink, T.D. Stack, *J. Inorg. Biochem.* 74 (1999) 138-149.
- [44] A. JahirUddin, F. J. Pawel, R. T. Minna, L. Makku, R. Timo, *Appl. Catal.* 371 (2009) 17-25.
- [45] M. Fabbrini, C. Galli, P. Gentili, D. Macchitella, *Tetrahedron Lett.* 42 (2001) 7551-7553.
- [46] E. G. Rozentsev, M. D. Goldfein, A. V. Trubnicov, *Usp. Khim.* 55 (1986) 1881-1897.
- [47] M. H. A. Janssen, J. F. Chesa Castellana, H. Jackman, P. J. Dum, R. A. Sheldon, *Green Chem.* 13 (2011) 905-912.
- [48] E. G. Rozentsev, E. S. Kagan, V. D. Scholle, V. B. Ivanov, V. A. Smirnov, In *Polymer Stabilization and degradation* P. Klemchuk (ed.), ACS, Symposium Series 280, Washington D. C. (1985) pp 11-45.
- [49] M. Yamaguchi, T. Miyazawa, T. Takata, T. Endo, *Pure Appl. Chem.* 62 (1990) 217-235.
- [50] P. Magnus, M.B. Roe, C. Hulme, *J. Chem. Soc., Chem. Commun.* 2 (1995) 263-265.
- [51] A. De Mico, R. Margarita, A. Mariani, G. Piancatelli, *Tetrahedron Lett.* 37 (1996) 1889-1892.
- [52] P. Gamez, I. W. C. E. Arends, J. Reedijk, R. A. Sheldon, *Chem. Commun.* (2003) 2414-2415.
- [53] B. Karimi, A. Biglari, J. H. Clark, V. Budarin, *Angew. Chem.* 119 (2007) 7348-7351.
- [54] B. Karimi, E. Farhangi, *Chem.-Eur. J.* 2011, 17, 6056-6060.

- [55] B. Karimi, E. Badreh, *Org. Biomol. Chem.* 9 (2011) 4194-4198.
- [56] P. Gamez, I.W.C.E. Arends, R.A. Sheldon, J. Reedijk, *Adv. Synth. Catal.* 346 (2004) 805-811.
- [57] W.A. Herrmann, J.P. Zoller, R.W. Fischer, *J. Org. Chem.* 579 (1999) 404-407.
- [56] A. Dijkman, I.W.C.E. Arends, R.A. Sheldon, *Chem. Commun.* 16 (1999) 1591-1592.
- [58] G. Yang, J. Ma, W. Wang, J. Zhao, X. Lin, L. Zhou, X. Gao, *Catal. Lett.* 112 (2006) 83-87.
- [59] A. Cecchetto, F. Fontana, F. Minisci, F. Recupero, *Tetrahedron Lett.* 42 (2001) 6651-6653.
- [60] R. Ben-Daniel, P. Alsters, R. Neumann, *J. Org. Chem.* 66 (2001) 8650-8653.
- [61] A. Dijkman, A. Marino-Gonzalez, A. Mairati i Payeras, I.W. C. E. Arends, R. A. Sheldon, *J. Am. Chem. Soc.* 123 (2001) 6826-6833.
- [62] M. F. Semmelhack, C. R. Schmid, D. A. CortNs, C. S. Chou, *J. Am. Chem. Soc.* 106 (1984) 3374-3376.
- [63] Scott D. McCann and Shannon S. Stahl, *Acc. Chem. Res.* 48 (2015) 1756-1766.
- [64] T. Karimpour, E. Safaei, A. Wojtczak, Z. Jagličić, A. Kozakiewicz, *Inorg. Chim. Acta* 395 (2013) 124-134.
- [65] G. Sheldrick, *Acta Crystallogr., Sect. A* 64 (2008) 112-122.
- [66] CrysAlis CCD171 and RED171 package of programs, Oxford Diffraction, 2000.
- [67] L. Hajikhanmirzaei, E. Safaei, A. Wojtczak, Z. Jagličić, *Inorg. Chim. Acta*, 430, (2015) 125-131.
- [68] L. Dutta, A. Syamal, *Elements of Magnetochemistry*, Affiliated East-West Press PVT LTD, (1993) 6-10.
- [69] C. Kittel, *Introduction to Solid State Physics* (8th Ed), John Wiley & Sons (2005)55-57.

- [70] E. Safaei, M. Mohseni Kabir, A. Wojtczak, Z. Jagličić, A. Kozakiewicz, Y.-I. Lee, *Inorg. Chim. Acta.* 366 (2011) 275-282.
- [71] X.-H. Bu, M. Du, Z.-L. Shang, L. Zhang, Q.-H. Zhao, R.-H. Zhang, M. Shionoya, *Eur. J. Inorg. Chem.* 2001 (2001) 1551-1558.
- [72] X.-H. Bu, M. Du, L. Zhang, Z.-L. Shang, R.-H. Zhang, M. Shionoya, *J. Chem. Soc., Dalton Trans.* (2001) 729-735.
- [73] M. Megnamisi-Belombe, M.A. Novotny, *Inorg. Chem.* 19 (1980) 2470-2472.
- [74] B. Karimi, F. Kabiri Esfahani, *Chem. Commun.* (2009) 5555-5557
- [75] S. E. Balaghi, E. Safaei, M. Rafiee, M. H. Kowsari, *Polyhedron* 47 (2012) 94-103.
- [76] S. E. Balaghi, E. Safaei, L. Chiang, E. W. Wong, D. Savard, R. M. Clarke, T. Storr, *Dalton Trans.* 2013, 42, 6829-6839.

## TEMPO-mediated Aerobic Oxidation of Alcohols using Copper(II) Complex of Bis(phenol) di-amine Ligand as Biomimetic model for Galactose oxidase Enzyme

Synthesis and characterization of copper complexes of  $N_2O_2$  bis(phenol) diamine ligands as models for Galactose oxidase and TEMPO-mediated aerobic oxidation of alcohols have been investigated.

